Available online at www.sciencedirect.com
SCIENCE DIRECT®
C. R. Physique 6 (2005) 683–692
COMPTES RENDUS PHYSIQUE
http://france.elsevier.com/direct/COMREN/

Interaction of electromagnetic fields with the environment/Interaction du champ électromagnétique avec l'environnement

Left-handed propagation media via photonic crystal and metamaterials

Thibaut Decoopman *, Thomas Crepin, Mathias Perrin, Sophie Fasquel, Aurélien Marteau, Xavier Mélique, Eric Lheurette, Olivier Vanbésien, Didier Lippens

Institut d'électronique de microélectronique et de nanotechnologie, université des sciences et technologies de Lille, avenue Poincaré, BP 60069, 59652 Villeneuve d'Ascq cedex, France

Available online 30 August 2005

Abstract

We review the electromagnetic properties of artificial structures such as photonic band gap materials (Electromagnetic Band Gap at microwaves) and metamaterials with main emphasis on backward (left-handed) propagation media. We consider free space and guiding structures by showing how the interaction of the electromagnetic wave with periodic dielectric (PBGs) and double negative metallic structures (DNGs) yields a negative refractive index. Some of the potential applications in connection with negative index media are briefly discussed such as focusing for a flat lens and phase advance for a left handed transmission line. ***To cite this article: T. Decoopman et al., C. R. Physique 6 (2005).***

Résumé

Propriétés électromagnétiques des milieux artificiels par des cristaux photoniques et des métamatériaux. Nous présentons les propriétés électromagnétiques de milieux artificiels tels que les matériaux à Bande Interdite Photonique (BIP) (ou Bande Interdite Electromagnétique en micro-ondes) et les métamatériaux, en particulier les métamatériaux main-gauche. Nous considérons des dispositifs en espace libre et des structures de guidage, et nous montrons comment l'interaction d'une onde électromagnétique avec des milieux diélectriques périodiques (BIP) et des milieux métalliques doublement négatifs conduit à un indice de réfraction négatif. Quelques-unes des applications potentielles en relation avec les milieux à indice de réfraction négatif sont brièvement présentées, telle que la focalisation par une lentille plane ou l'avance de phase pour une ligne de transmission main-gauche. ***Pour citer cet article : T. Decoopman et al., C. R. Physique 6 (2005).***

1. Introduction

Photonic (Electromagnetic) Band Gaps (PBGs /EBGs) and metamaterials are periodic structures, patterned on a scale comparable or much shorter than the operating wavelength. The relevant dimensions are thus on a nanometer scale if infrared or visible spectra are targeted. Even though they are made of positive index materials, these structures exhibit abnormal dispersion characteristics in the long wavelength regime. The materials can indeed exhibit a strong anisotropy, or behave as a medium of negative index of refraction—associated with negative values of the permittivity and permeability.

* Corresponding author.
E-mail addresses: Thibaut.Decoopman@fresnel.fr (T. Decoopman), Didier.Lippens@iemn.univ-lille1.fr (D. Lippens).

1631-0705/$ – see front matter
doi:10.1016/j.crhy.2005.06.007

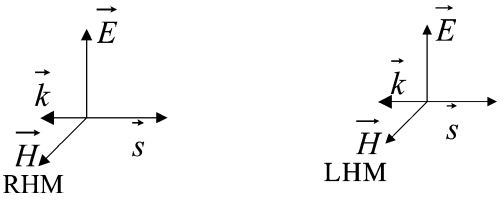

Fig. 1. (E, H, K) trihedrons for Left-Handed (LH) and Right-Handed (RH) materials.

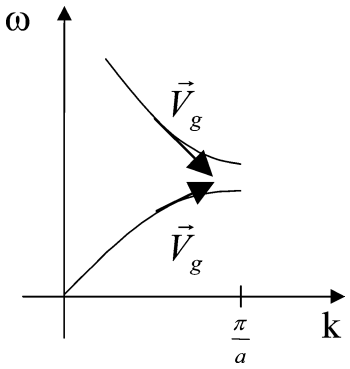

Fig. 2. Illustration of the left-handed character of the second branch.

In such double negative (DNG) media, propagation of light, or generally of electromagnetic (EM) waves can be backwards. The wave vector, **k**, electric field, **E**, and magnetic field, **H**, constitute an indirect trihedron, where **k** and the Poynting vector, **S**, are antiparallel (Fig. 1). In this case, they are termed Left-Handed Materials (LHMs) as proposed by Veselago in 1968 [1].

Beyond this inversion of phase velocity with respect to the direction of energy flow, an impact of a negative refractive index, n, may be found in negative refraction. The incident and refracted beams are then on the same side of the normal to refraction interface, as it is predicted by the Snell–Descartes law, with a negative refractive index. It results in a natural focusing effect with flat lenses (Veselago lens), whose properties are invariant by translation, with the prospect, as proposed recently by Pendry [2], to also avoid the diffraction limit with the so-called 'superlens effect' (ideal lens).

In this paper, we address the general problem of the interaction of an EM wave with such micro and nanostructures, with the main emphasis on the effects in connection with a negative refractive index. First, we show how the lefthandedness can be pointed in DNG media via (i) band structure calculation assuming Bloch waves, and (ii) the comparison of phase shift in finite EM region of various lengths. Then we focus on dielectric periodic structures by considering mainly 2D structures whereas, in the last sections, we address the main issue in connection with metamaterials made of dielectric and metal composites. Technological challenges for fabricating real life prototypes will be shortly discussed when specific technological developments have to be solved.

2. Lefthandedness signature

It is well known that gaps may be open in a periodic structure. The simplest electromagnetic device of this kind is the so-called Bragg reflector made of various alternate layers with different refractive index. The forbidden gap corresponds in this case to the reflectance plateau resulting of the constructive interference of the various components of the reflected wave at the interfaces. The thickness of each layer has to match a quarter of the wavelength in the considered medium and thus the pertinent scale (pitch of this one D-periodic structure) is comparable to the operating wavelength. In the gap, the EM waves are evanescent and thus the propagation is forbidden. Out of this gap, propagation can take place with dispersion effects due to the openness of this gap. For the lower frequency dispersion branch the propagation is right-handed, as illustrated in Fig. 2. The group velocity (v_g) and the phase velocity ($v\varphi$) have the same direction whereas the dispersion branch above the gap is left handed with v_g and v_φ of opposite sign. This is the first signature of the left-handed character of a dispersive propagation media. It is based on the consideration of an infinite propagation medium defined by a unit cell with a characteristic dimension (a) defining by this means the boundary of the Brillouin zone.

Let us consider first a dielectric array of holes etched in a high index dielectric. Fig. 3 shows a Scanning Electron Micrograph (SEM) of such a 2D hole array patterned in a Si_3N_4 thin film which will be used for subsequent deep etching by RIE. This nanostructure, fabricated at IEMN, was patterned by e-beam lithography using conventional PMMA resist, Plasma Enhanced Chemical Vapor deposition (PECVD) for the transfer of a Si_3N_4 layer and Deep Reactive Ion Etching for the dry etching of holes.

Fig. 4 illustrates the etching stage. The structure under test is based on an InP technology with conventional technique to confine the light in the direction perpendicular to the growth axis of semiconductor (namely the use of InGaAsP/InGaAs heterojunction). Despite the high filling factor between air and semiconductor the high degree of anisotropy afforded by the reactive plasma etching technique permitted us to etch holes with a typical diameter around 0.3 μm with comparable period

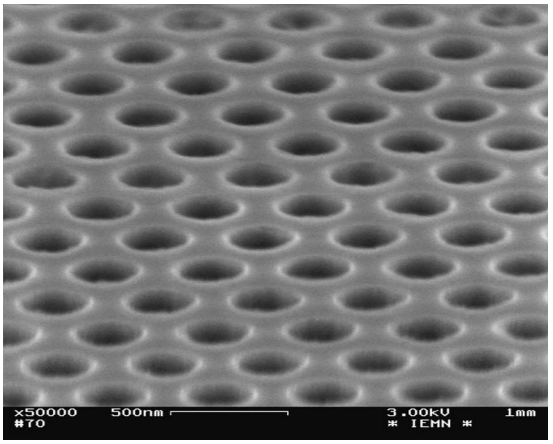

Fig. 3. Scanning electron micrograph of a hole area.

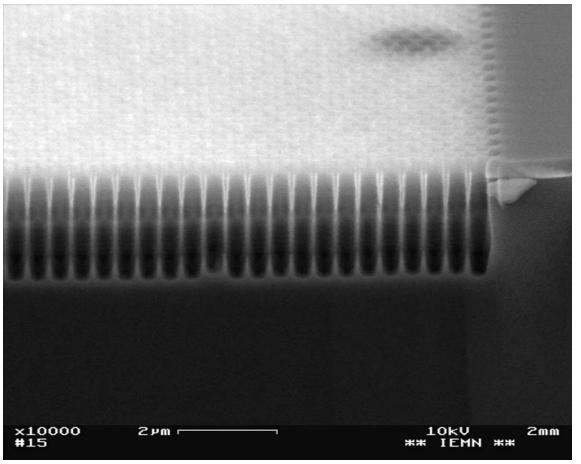

Fig. 4. Scanning Electron Micrograph of a 2D photonic crystal.

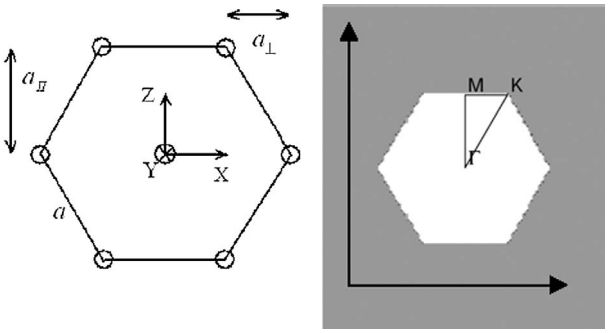

Fig. 5. Schematic of the hexagonal dielectric structure with the definition of main direction in the Brillouin zone.

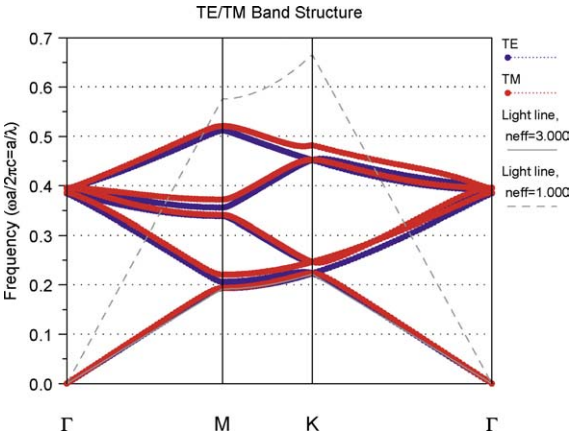

Fig. 6. Dispersion characteristic of a hexagonal hole array for TE and TM polarizations.

and a depth of 3 µm. High aspect ratio nanostructures (10 : 1) are thus successfully fabricated on a deep submicron technology (relevant dimensions around a few hundred of nanometers).

Turning now to a generic hexagonal structure with an index contrast $\Delta n = 2$, whose geometry is schematised in Fig. 5 along the main direction in the Brillouin zone, ΓM, ΓK and KM respectively. The air filling factor we considered in the present example is $f = 0.093$.

The corresponding band structure is shown in Fig. 6, for both TE (field components Hx, Ey, Hz) and TM (field components Ex, Hy, Ez).

The dispersion relation of the photonic structure—band diagram—has been obtained using commercial software, BandSolve, developed by Rsoft. A Matlab code has also been developed, and used for the same purpose. More generally, note that several numerical methods may be used to solve the numerical problem, and find the couple $(\omega, \vec{k})$ to define the dispersion relation of a plane wave propagating in an infinite medium. The core of the problem is the resolution of an eigenvalue equation: $M_k \Phi = \lambda_k \Phi$, where $\lambda_k = (\omega/c)^2$, and,

$$M_k = (\nabla + i\vec{k}) \wedge \left[\left(1/\varepsilon(r)\right)(\nabla + i\vec{k})\right] \wedge,$$

where $\wedge$ is the vectorial product.

We have used a numerical procedure based on Hessenberg decomposition and a QR method to solve the linear system that gives the eigen elements. Such a method requires the computation of all the matrix elements, which is not too serious a problem, provided one avoids 3D simulations. It has been shown that convergence problems may occur with such an algorithm [3]. In that case, one shall use a fine evaluation of the Fourier transform of $1/\varepsilon$ [4], or variational methods [5–7]. However, in our

case, considering around 10^3 plane waves has been enough to model accurately the band structure. We also have carried out time domain simulations: two-dimensional FDTD, using FullWAVE, by Rsoft. This algorithm directly integrates the Maxwell propagation equations using finite difference method.

Due to the small filling factor—small air holes—the first band is very close from the light line of a homogeneous medium of index $n_{\text{hom}} = 2.81$. This corresponds to the average of the permittivity of air and dielectric, weighted by their surfacic fraction. No gap is present here, and thus the higher order bands appear for quite low frequency: $a/\lambda > 0.2$.

The components of group velocity: $Vg_i = \partial\omega/\partial k_i$, with $i = \{x, z\}$, are positive on the first ground band. Conversely, they can take negative values on higher energy bands.

In order to give a more precise look at the prediction concerning propagation in such a bi-dimensional crystal, one has to get out of the 1D-picture and look at the energy contours in the Brillouin zone.

An example of such a mapping of iso-frequency contours is reported in Fig. 7. Close to the Γ point the dispersion properties are quite isotropic circle-like energy contours. In contrast anisotropy effects can be found close to the boundary of the Brillouin zone. For applications in imaging, it will be very important to work in the zones of isotropy, as all the rays coming from one source will experience the same index of refraction. This reasoning is thus different from those invoked for ultra-refraction effects where conversely a high anisotropy is a welcome feature.

Until now, we have presented results valid for infinite structures, where plane waves propagate. Let us now focus on a real device of finite size, where diffraction at the input can occur and be a new origin of anisotropy. Consider here a vacuum wavelength corresponding to $a/\lambda = 0.28$, and compare what happens for directions ΓM (second band), and MK (third band), for TM polarisation. For a hexagonal structure, the step of the grating in both direction MK and ΓM $- a_{\text{II}} = 0.24\lambda$ and $a_{\perp} = 0.14\lambda$, respectively—is not the same.

Thus, a beam coupling from free space will not be diffracted in the same way for both directions. The more intense diffraction in the case of an input along MK will create wavefronts along other directions—cf. Fig. 8(a). On the contrary, Fig. 8(b) shows that the beam propagates with few perturbations. One can conclude that anisotropy effects are twofold: for infinite material, they appear in the band structure (Fig. 6), for finite size systems, diffraction at the entrance/output also plays a role.

If optical devices were made of this material, image limitations due to diffraction would strongly depend on the direction of input, and thus be more complex than what arises with ordinary materials. It is therefore important to work in a frequency range, where the medium behaves isotropically, as if it was homogeneous.

Fig. 9 illustrates the refraction regime for a wave impinging onto a prism like-dielectric array. The feeding of the structure is along the ΓM direction. The frequency of the EM wave is chosen in the Left Handed dispersion branch by taking care to preserve the isotropy, working close to Γ. By analysis of the phase front it can be seen that the—large arrow—beam refracts on the other side of the normal—dashed line—compared to a conventional positive refractive index materials.

Fig. 10 shows the results of a numerical experiment showing focusing of EM waves by means of a flat lens. The source consists in a truncated waveguide on the left hand side of the figure, close to the lens made of the artificial structure. A first focus is apparent within the composite slab and another can also be seen on the other side of the lens. Such a focusing effect, making use of negative refraction, is invariant by translation in contrast to conventional lenses.

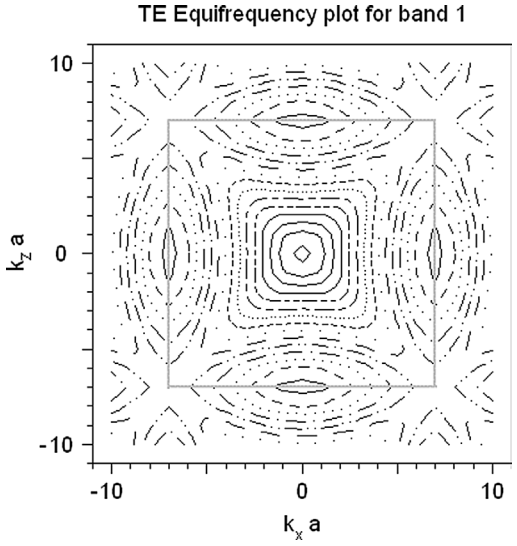

Fig. 7. Iso-frequency (energy plot) in the Brillouin zone.

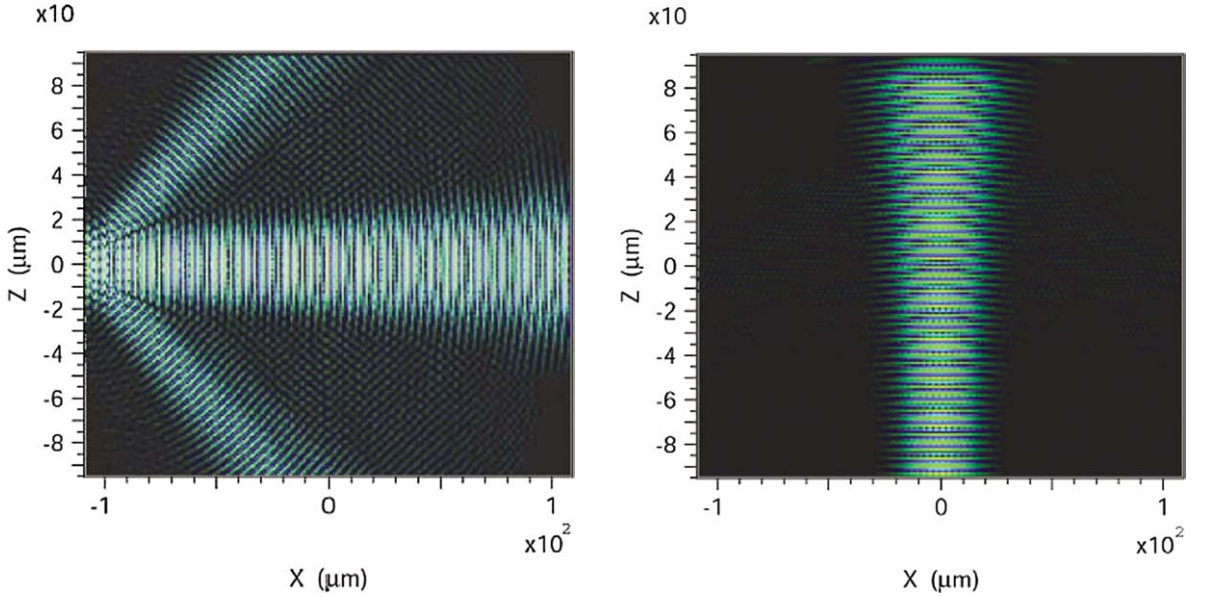

Fig. 8. (a) Component Hy inside a 2D periodic structure for injection along the MK direction (TM polarization $a/\lambda = 0.28$); (b): Input along the ΓM direction.

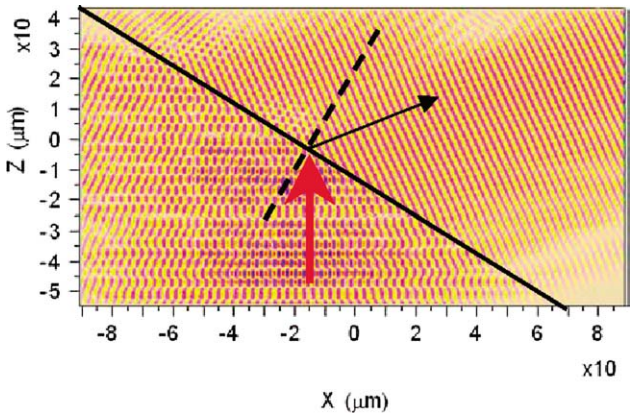

Fig. 9. Numerical modelling of the negative refraction effect.

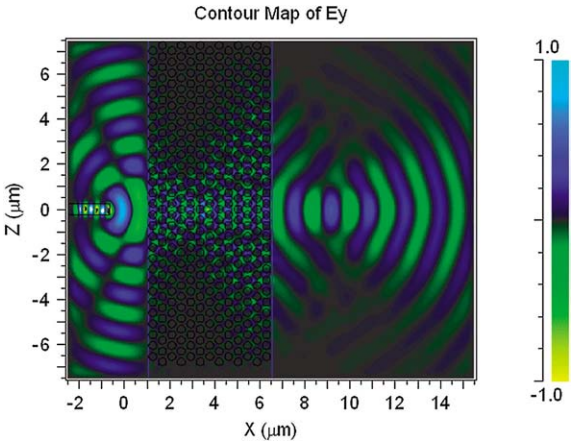

Fig. 10. Illustration of the focusing effect in a 2D flat lens (Veselago lens).

Using the view of the negative refraction of incident beams, it is also possible to have a first estimate of the effective refractive index of the lens. From Snell–Descartes law in the present numerical experiment a value close to unity is thus not far from the ideal situation where perfect matching is obtained.

3. Metamaterials: SRR and wire arrays

The prefix ‘meta’ means beyond. Indeed, by a proper structuring of materials, the possibility to synthesize double negative media can be demonstrated and notably artificial media exhibiting a negative permittivity value, created by wires arrays. This approach was inspired by plasma physics with the key result that a resonant behaviour of free carriers can be obtained at the plasma frequency [8]. Below this frequency, the effective permittivity is negative. For a metal, this frequency is in the UV range, but can be lowered to microwave region by dramatically decreasing the filling factor of wire arrays embedded in a dielectric

host substrate. With this aim, one possibility is to use thin metallic wire grids arranged in a periodic way. In this case, the electron density is strongly decreased, such as the plasma frequency. Fig. 11 shows the scattering parameters (S_{ij}) obtained for Aluminum wires with a radius of 1 µm, separated by 5 mm. This media is excited with a plane wave, electrically polarized along the wires. Below 11 GHz, the permittivity becomes negative and the transmission drops.

To allow EM propagation, permeability has also to be negative, simultaneously. This can be achieved with metallic open rings, such as those first proposed by Pendry and termed as Split Ring Resonators (SRR) [9]. It is worth noting that a magnetic response is thus obtained with current loops made from non magnetic materials. Basically, the principle is to combine inductive and capacitive effects to create a resonance leading to a negative permeability. Fig. 12 is an optical view of various magnetic particles fabricated by e-beam lithography at IEMN. Square- or ring-shaped elements can be designed and their relevant dimensions permit one to tailor the frequency of operation by changing the resonance frequency which is also characterized by a high quality factor.

In conventional operation, in order to properly excite the SRR, the incident magnetic field has to be perpendicular to the plane containing the ring. However, recently it was shown SRRs that can be excited (existence of current loop when the electric field is parallel to a gap bearing arm of the SRR) [10]. The main drawback of the SRR is the limited bandwidth, since the effective permeability is negative in a narrow frequency band between the resonance frequency of the current loops and the magnetic plasma frequency.

To increase the operation frequency range, simple scaling rules can not be applied keeping in mind that other phenomena such as electron inertia and edge effects have also to be considered. Nevertheless, this kind of resonant and metallic ring is expected to operate at least up to mid-infrared. With this aim, other submicronic shapes are investigated to circumvent the aforementioned limitations. Fig. 13 is an optical microscope view of recent structures fabricated at IEMN for infrared operation.

To create a double negative media (DNG), wire and SRR arrays are superimposed [11]. Even if the magnetic and electrical responses are coupled, it is possible to keep the magnetic resonance in a frequency range where the permittivity is negative. Another key point concerns the coupling of this artificial media with free space. Indeed, careful impedance matching has to be achieved to prevent reflection at the interface and thus minimize the return losses. Under these conditions, the transmissivity can be close to unity in the frequency range where both permittivity and permeability are simultaneously negative and the

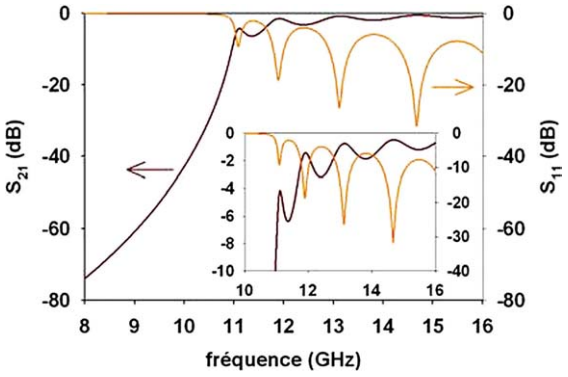

Fig. 11. Electromagnetic response of an aluminum wire array.

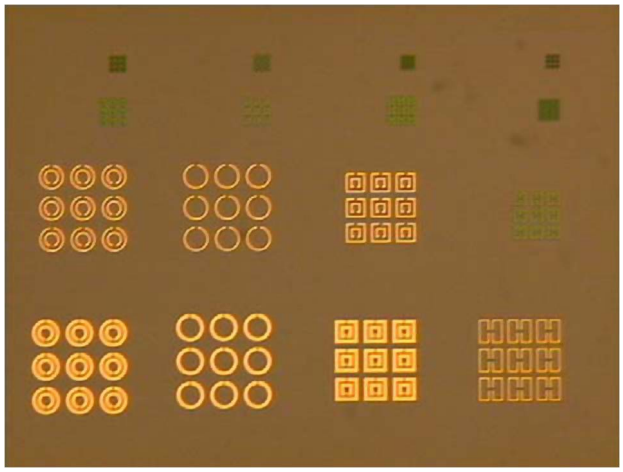

Fig. 12. Optical view of the various SRR (Split Ring Resonators) arrays.

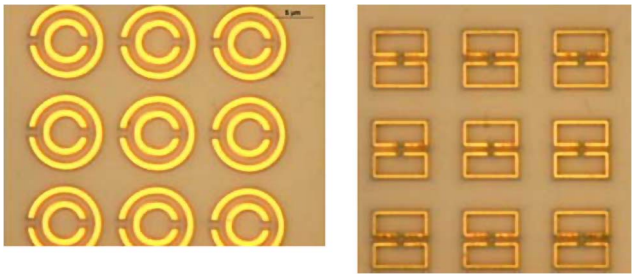

Fig. 13. Enlarged views of two kind of SRRs for operation in infrared.

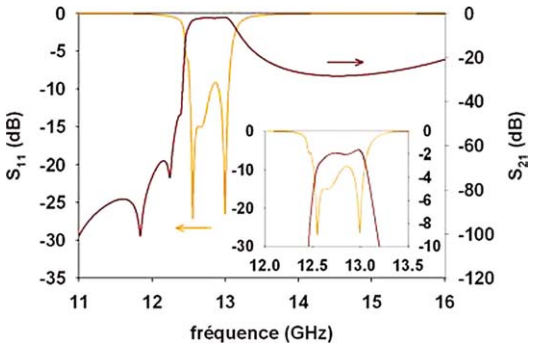

Fig. 14. Full-wave analysis of a DNG array operating in X band.

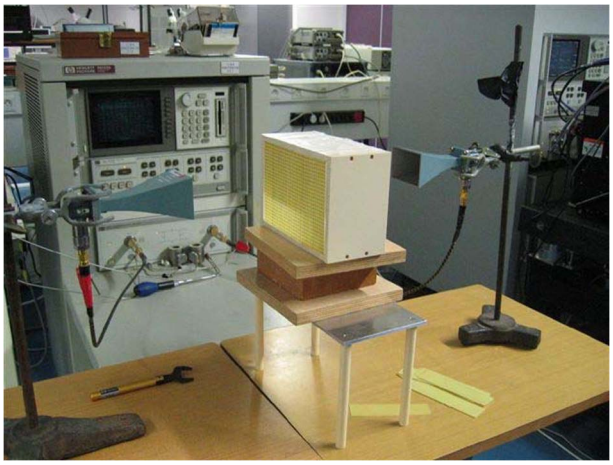

Fig. 15. View of the experimental set up for the frequency assessment of free space prototypes. The SRR array is placed here in order to have the electric field parallel to a gap bearing arm of SRRs.

impedances are equal [12]. Fig. 14 shows the frequency dependence of the scattering of a prototype operating at X band. The device is left-handed between 11.5 and 13.5 GHz with a maximum of transmission around −2 dB.

The free space experimental setup used for the characterization is presented Fig. 15. In the present experiment we assessed the frequency response of a SRR array with the incident electric field parallel to the gap bearing arm. The medium is probed by means of horns, which are used to generate a quasi planar wave. The characterization is conducted by means of vectorial network analysis and we will see in the following section that such experiments allow the experimental assessment of the left handed character.

4. Left-handed transmission lines (finline technology)

For microwave applications, the transmission line approach is more appropriate for circuit design and integration in existing systems. High performance coupling, phase-shifting or filtering devices can be thus fabricated, benefiting from a sub-wavelength structured left-handed medium with the associated benefit of high compactness. In this context, the finline technology is a good candidate and we present in this section the analysis of a novel left-handed composite transmission line that we proposed recently [13].

This one-dimensional propagation structure is based on the dual transmission line configuration. Indeed by inverting reactive elements in order to have a series capacitance and a shunt inductance, it is possible to obtain a highly dispersive left-handed transmission line. Practically, this topology is difficult to realize, but it is possible to load periodically a classical line with discrete elements. In this case, the dispersion diagram is modified and exhibits a frequency bandwidth within the propagation which is left-handed. In this work, the main waveguide is a finline, consisting in a slotline inserted in the E-plane of a metallic hollow waveguide. Such a transmission line is periodically loaded with thin wires in a shunt configuration. Instead of series resistance ring resonators are patterned on the backside of the substrate (Fig. 16). The period and a fortiori the characteristic dimensions of wires and SRR's are small compared to the guided wavelength, in order to allow the homogenisation of the medium. From the modeling side, the band diagram can be deduced from the scattering parameters of an unit cell, calculated

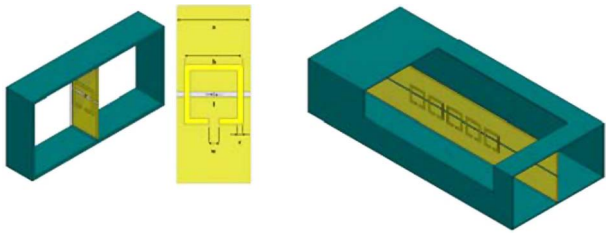

Fig. 16. Basic cell and schematic of a LH transmission line.

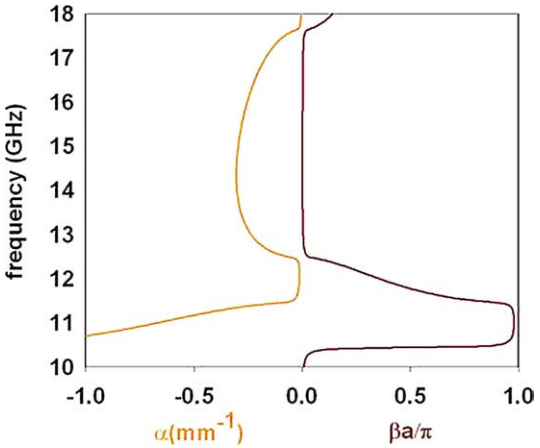

Fig. 17. Band structure of the transmission line in a finline technology.

Fig. 18. Photo of a Ka band LH finline.

with a finite element method (HFSS by Ansoft). This diagram shows a band pass between 11.5 and 12.5 GHz (Fig. 17), with a negative slope, indicating that the wave vector and the Poynting vector are opposite in sign as discussed in introduction. The propagation is thus backward, since the wave front moves in an opposite direction with respect to that of energy. Numerically, this backward propagation can be demonstrated by time domain analysis or by modifying the phase at the origin in order to mimic a temporal analysis. Fig. 18 shows a photo of a Ka band prototype (10–18 GHz), consisting in 20 unit cells. The metallic waveguide is split and machined to allow planar circuit housing inside a groove.

The ring resonators on the picture were fabricated by conventional Printed Circuit Board techniques, and the prototypes were characterized by means of vectorial network analysis. These measurements have shown low insertion losses, indicating a good impedance matching between the composite transmission line and the embedding media (waveguiding section). The metallic shielding afforded by the waveguide prevents any radiation losses. Under this condition the transmission losses can be linked to the use of highly resonant metallic rings and a trade-off has to be found between the level of rejection and the overall losses.

A direct experimental verification of the lefthandedness of this structure can be found from the phase offset between two lines of various lengths. It can be shown that this offset ($\Delta\phi$) is positive when propagation is backward and negative for a right handed behaviour. Fig. 19 shows the variation versus frequency of $\Delta\phi$ measured and calculated for the device under test. In the left handed dispersion branch $\Delta\phi$ is positive in agreement with the band structure calculation.

5. Periodically loaded C–L transmission lines

As shown before LH propagation media can be realized with transmission lines periodically loaded by quasi-lumped elements. In this section we present a coplanar strip (CPS) transmission line approach using Metal Insulator-Metal-capacitors and meander-like inductors. The first originality with respect to the literature is their frequency of operation in the Terahertz range while to the state of the art, works address the microwave range. The second novelty is the characterization method we used which is based on electro-optic sampling experiment.

Fig. 20 is an optical view of the devices which were designed and fabricated following these guide lines. The Coplanar stripline (CPS) is composed of two planar metallic conductors patterned on a substrate. On such a line, with two separate conductors, the propagation mode is quasi-TEM.

With the C–L type scheme loading the line, the electromagnetic wave interacting with the structure will see a series of C–L high-pass sections. It can be shown that the ground dispersion branch is left handed. According to the criterion of metamaterials, the physical dimensions of components have to be small with respect to the wavelength. In practice we chose the following parameters. The width of the strips is 10 μm and the distance between both strips is 25 μm. The capacitors are parallel-plate capacitors with 100 μm^2 area and 300 nm Si_3N_4 dielectric. To extend the inductance value we design a meander strip. This strip has a 200 μm total length and a 200 nm width. The periodicity is about 30 μm. Full wave analysis shows the first transmission band is centered around 200 GHz and the bandwidth is approximately 200 GHz (Fig. 21). From the technological point of view the meander inductances were patterned by e-beam lithography, and the parallel plate capacitors were fabricated by PECVD dielectric deposition.

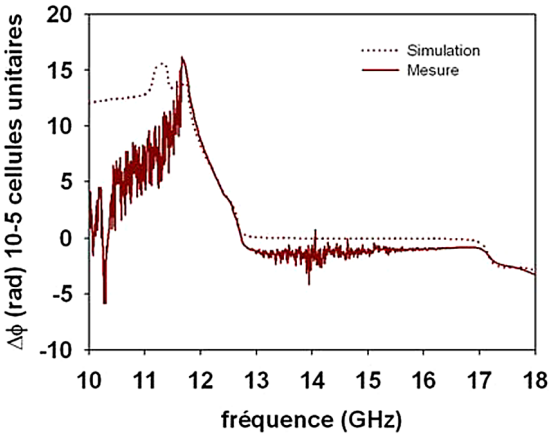

Fig. 19. Experimental evidence of lefthandedness via the phase offset between two lines.

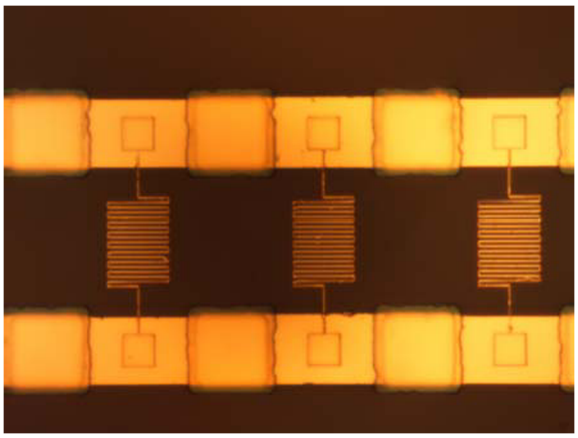

Fig. 20. Photo of the C–L type LH transmission line operation at Terahertz frequencies.

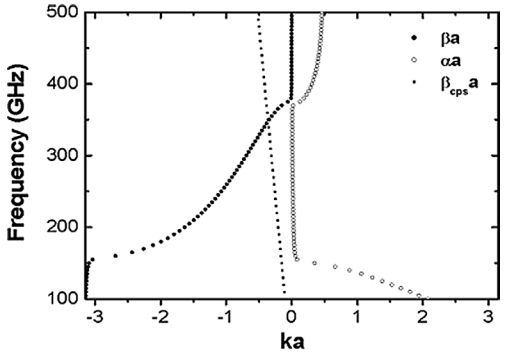

Fig. 21. Band structure calculation of the C–L type LH transmission line.

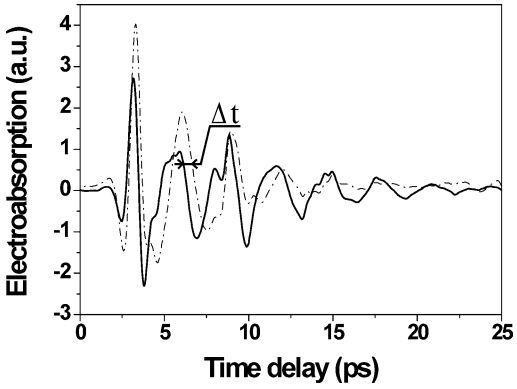

Fig. 22. Time dependence of the transmitted signal through the devices. Experimental evidence of the phase advance (21 cells solid line, 17 cells dashed line).

In order to generate ultra short pulses, the lines are covered with patches of low temperature grown semiconductor. Electro-optic sampling is carried out in a pump probe experiment with GaAs thin film for the generation and AlGaAs ones for the probing of the transmitted and reflected wave. For the latter, we record the variations of electro-absorption by Franz Keldish effect.

Fig. 22 shows the time variation of the transmitted pulse for a 21 cells and 17 cells transmission lines. There is a phase advance for the former resulting from the backward propagation.

6. Conclusion

Left-handedness of various metamaterial-based EM propagation media is now demonstrated theoretically and experimentally. This can be seen through the band structure calculation numerical experiment of the negative refraction and the focusing by flat lenses or by monitoring the phase offset by frequency or time domain analysis. Beyond the improvement of intrinsic performance notably by addressing the losses issue, the next stages are nanostructring of 3D devices and the investigation of new routes for negative permeability.

Acknowledgements

This work has been carried out in the framework of the Network of excellence METAMORPHOSE, the Eureka project TELEMAC and the coordinated research projects in the framework of Nanosciences and Nanotechnology French programme (ACI NANOTHEME and METAPHORE).

References

[1] V.G. Veselago, The electrodynamics of substances with simultaneously negative values of ε and μ, Sov. Phys. Uspekhi 10 (4) (1968).
[2] J.B. Pendry, Negative refraction makes a perfect lens, Phys. Rev. Lett. 85 (18) (2000).
[3] H.S. Sozuer, J.W. Haus, R. Inguva, Photonic Bands: Convergence problems with the plane-wave method, Phys. Rev. B 45 (1992) 13962.
[4] R.D. Meade, A.M. Rappe, K.D. Brommer, J.D. Joannopoulos, O.L. Alerhand, Accurate theoretical analysis of photonic band gap material, Phys. Rev. B 48 (1993) 8434.
[5] S.G. Johnson, J.D. Joannopoulos, Bloch-iterative frequency-domain methods for Maxwell's equations in a planewave basis, Optics Express 8 (2001) 173.
[6] A. Edelman, S.T. Smith, On conjugate gradient-like methods for eigen-like problems, B.I.T. 36 (1996) 494.
[7] M.C. Payne, M.P. Tater, D.C. Allan, T.A. Arias, J.D. Joannopoulos, Iterative minimization technique for ab-initio total-energy calculations: molecular dynamics and conjugate gradients, Rev. Mod. Phys. 64 (1992) 1045.
[8] J.B. Pendry, A.T. Holden, W.J. Stewart, I. Youngs, Extremely low frequency plasmons in metallic mesostructures, Phys. Rev. Lett. 76 (1996) 4773.
[9] J.B. Pendry, A.J. Holden, D.J. Robbins, W.J. Stewart, Magnetism from conductors and enhanced nonlinear phenomena, IEEE Trans. Microwave Theory Tech. 47 (11) (1999).
[10] R. Marques, F. Mesa, J. Martel, F. Medina, Comparative analysis of edge- and broadside-coupled split ring resonators for metamaterial design. Theory and experiments, IEEE Trans. on Antennas and Propagation, in press.
[11] R.A. Shelby, D.R. Smith, S.C. Nemat-Nasser, S. Schultz, Microwave transmission through a two-dimensional, isotropic, left-handed metamaterial, Appl. Phys. Rev. Lett. 78 (2001).
[12] C.G. Parazzoli, R.B. Greegor, K. Li, B.E.C. Koltenbah, M. Tanelian, Experimental verification and simulation of negative index of refraction using Snell's law, Phys. Rev. Lett. 90 (2003) 107401.
[13] T. Decoopman, O. Vanbésien, D. Lippens, Demonstration of a backward wave in a single split ring resonator and wires loaded finline, IEEE Microwave and Wireless Components Lett. 14 (11) (2004).